

**Chemical and structural characterization of fibrous richterite with high environmental and health relevance from Libby, Montana (USA)**

Alessandro Pacella* and Paolo Ballirano

Dipartimento di Scienze della Terra, Sapienza Università di Roma, Piazzale Aldo Moro, 5 - I-00185 Roma, Italy

ARTICLE INFO

Submitted: February 2016

Accepted: April 2016

Available on line: June 2016

* Corresponding author:

alessandro.pacella@uniroma1.it

DOI: 10.2451/2016PM638

How to cite this article:

Pacella A. and Ballirano P. (2016)

Period. Mineral. 85, 169-177

ABSTRACT

This study reports new structural and spectroscopic data of a sample of fibrous richterite from Libby, Montana (USA). The OH-stretching region was investigated by FT-IR. The spectrum showed, except for the typical absorption band at 3671 cm⁻¹ assigned to the vibration of the O-H dipole bonded to three ^[6]Mg cations, a well developed band at 3658 cm⁻¹ attributed to the ^{M(1)+M(3)}Fe²⁺ environment. The ^{M(1)+M(3)}Fe²⁺ occupancy calculated using the FT-IR data is in very good agreement with that obtained combining Mössbauer and EMP data. Fe³⁺ was only assigned at *M*(2) owing to the absence in FT-IR spectrum of absorption bands at $\Delta= -50$ cm⁻¹ from the tremolite reference band. Structural investigation was done by X-ray powder-diffraction using the Rietveld method. Cell parameters, fractional coordinates for all non-hydrogen atoms, and site scattering for *M*(1), *M*(2), *M*(3), *M*(4) and *A* were refined. The most relevant difference with respect to prismatic winchite is a general reduction of the cell parameters that is ascribed mainly to the higher fluorine content of fibrous richterite. Possible site occupancies were obtained by combining chemical data and Rietveld refinement results.

Keywords: Fibrous richterite; winchite; Libby; XRPD, Rietveld method; FT-IR.

INTRODUCTION

Since 1999, the small town of Libby, Montana (USA) has been involved in one of the most significant asbestos issues in the Northern America. A high incidence of asbestosis, lung cancer, and mesothelioma cases (McDonald et al., 1986; 2001) was found in miners and millers who worked in a vermiculite mine situated near the town of Libby that was operated from 1923 to 1990 for the local building industry. Vermiculite, after being mined and concentrated, was expanded by rapid heating to form Zonolite, a commercial product that was widely used in many consumer products such as fireproofing materials, absorbents and industrial fillers. The mine is located in the Rainy Creek complex, a Cretaceous alkaline-ultramafic igneous body, essentially consisting of a biotitite core, surrounded by a ring dyke of biotite pyroxenite, which is in turn surrounded by a magnetite pyroxenite (Gunter et al., 2003). Biotite in the biotite pyroxenite was altered to vermiculite by low-temperature weathering, and pyroxenes were altered to

amphiboles by a higher-temperature hydrothermal process (Boettcher, 1966). Amphiboles in the altered areas can reach concentrations from 50 to 75% and are intimately associated with other phases such as talc, titanium oxides, pyrite, limonite, calcite, K-feldspar, quartz and albite (Pardee and Larsen, 1928). Careful mineralogical investigation (Wylie and Verkouteren, 2000; Gunter et al., 2001; 2003; Meeker et al., 2003; Sanchez et al., 2008;) showed the occurrence of fibrous amphibole in the vermiculitic deposits, with compositions ranging from richterite to winchite. As a consequence, the environmental survey finally related the cases of diseases to the occurrence of asbestiform richterite and winchite. Interestingly, both minerals are currently unregulated as asbestos. Toxicological studies provide clear evidence that the interactions between fibrous material and biological environment are strongly dependent on both the geometry and the crystal chemistry of mineral fibres (Fubini, 1993; 1996; Fubini and Otero Aréan, 1999). In particular, the presence and bioavailability of Fe has received

considerable attention from the biomedical community. Both the presence and the structural coordination of iron were proposed as important factors in the toxicity of asbestos (Fubini et al., 2001). Recently, Pacella et al. (2015) showed that, for fibrous amphiboles, chemical reactivity seems to be related not only to iron content and oxidation state on the surface, but also to its nuclearity and surface-alteration mechanisms. Morphostructural/biological activity relations in fibrous minerals are a crucial subject still to be clarified, and a detailed chemical and structural investigation of the fibres is the fundamental first step.

In the present work, we report for the first time a full structural and spectroscopic characterization of a sample of fibrous richterite from Libby, Montana (USA). Cation site partition has been obtained from chemical and Mössbauer data already reported in Fantauzzi et al. (2012) and new FT-IR and X-ray powder diffraction data.

ANALYTICAL METHODS

Scanning Electron Microscopy (SEM)

SEM was done using a Philips XL30 equipped with an EDAX system for EDS microanalysis. Images were obtained from a fragment of the hand specimen mounted on a sample stub and carbon coated. Analytical conditions were: 15 kV accelerating voltage, 10 mm working distance and a tilt angle of 0°. Electron micrographs showing the fibrous morphology at different magnifications are shown in Figure 1.

Fourier-Transform InfraRed (FT-IR) Spectroscopy

FT-IR data were collected on a Nicolet MAGNA 760 over the range 4000-400 cm^{-1} : 32 scans at a nominal

resolution of 4 cm^{-1} were averaged. The instrument was equipped with a KBr beamsplitter and a TGS detector. The powdered samples were mixed in a 2:100 ratio with 200 mg of KBr in order to obtain transparent pellets. Measurements were done in air at room temperature. The spectrum (Figure 2) was fitted using the PEAKFIT program (Jandel Corporation); the background was modelled using a linear function and, the peaks were modelled using symmetrical Gaussian line-shapes. Table 1 lists the values of the calculated wavelength, FWHM and intensity of each absorption peak.

X-ray Powder Diffraction (XRPD)

XRPD data were collected on a fully automated parallel-beam Bruker AXS D8 Advance diffractometer, operating in transmission mode, equipped with a Position Sensitive Detector (PSD) VANTEC-1. Fibres were ground under ethanol in an agate mortar and the powder mounted in a 1 mm diameter borosilicate glass capillary. Preliminary evaluation of the diffraction pattern indicated the presence of small amounts of microcline that has been included in the refinement. Rietveld refinement was done with GSAS crystallographic suite of programs (Larson and Von Dreele, 1985) using the EXPGUI graphical user interface (Toby, 2001). The background was fitted with a 32-term Chebyshev polynomial of the first kind to model the amorphous contribution arising from the capillary. Peak shape was fitted using a TCH pseudo-Voigt function (Thompson et al., 1987) modified for asymmetry (Finger et al., 1994). Refined parameters were GU ($\tan^2\theta$ -dependent), GV ($\tan\theta$ -dependent), GW (angle-independent) Gaussian parameters, LX (1/ $\cos\theta$ -dependent) Lorentzian parameter,

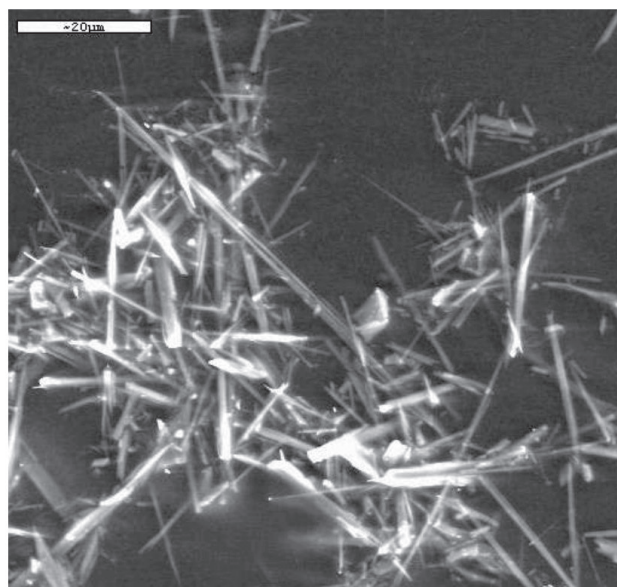
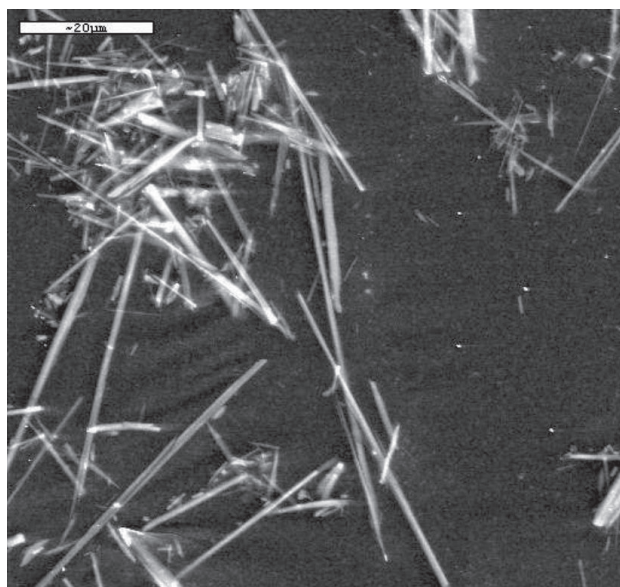


Figure 1. SEM images of fibrous richterite from Libby. Dimension bar 20 μm .

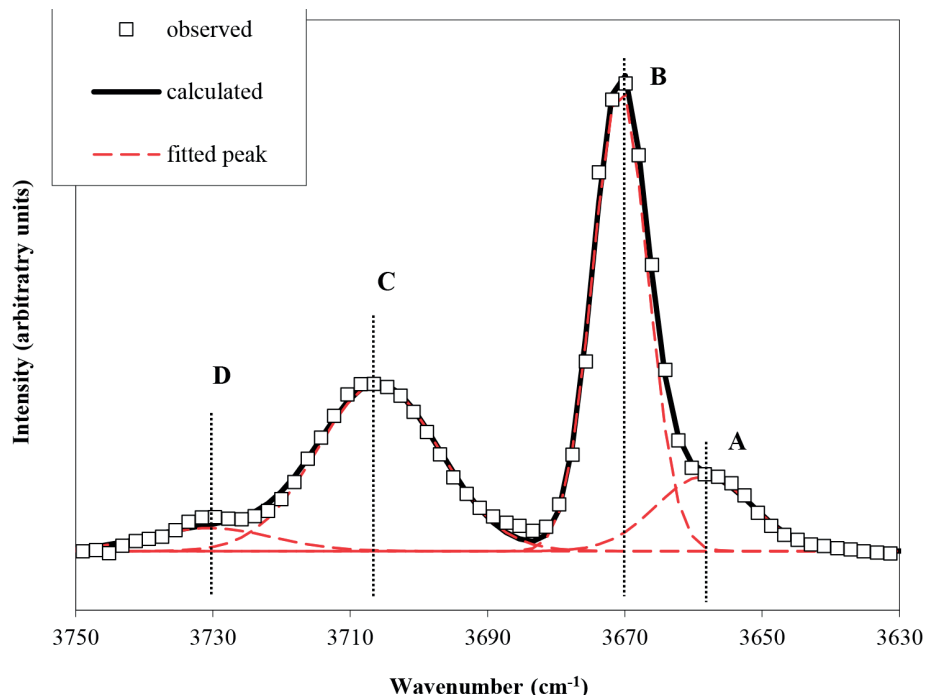


Figure 2. FT-IR spectrum of the OH stretching region of fibrous richterite from Libby.

Table 1. Fitted and calculated FT-IR data for fibrous richterite from Libby.

Band	Position (cm ⁻¹)	Width (cm ⁻¹)	Intensity (%)
A	3658	16	9
B	3671	9	30
C	3706	21	54
D	3731	22	7

and S/L and H/L asymmetry parameters (constrained to be equal in magnitude). Refinement of two independent scale-factors for amphibole and microcline allowed quantitative analysis of the mixture. Starting structural data were those of Gunter et al. (2003) for the amphibole and those of Allan and Angel (1997) for microcline. Cell parameters were refined for microcline, whereas fractional coordinates for all atoms and site scattering for $M(1)$, $M(2)$, $M(3)$, $M(4)$ and A were also refined for the fibres. Attempts to independently refine the position of the $A(2)$ and $A(m)$ sites failed because of the correlation with the adjacent A site. This behaviour is consistent with that observed by Hawthorne et al. (2008) for richterite, whose difference-Fourier map through the $A(2/m)$ site calculated after removal of the A cations indicated single centre of maximum density at the $A(2/m)$ site. Therefore, a single site $A(2/m)$ (special position 0, $\frac{1}{2}$, 0) was considered during the refinement. The isotropic

displacement parameters were kept fixed throughout the refinement to the values refined for prismatic winchite (Gunter et al., 2003) because of the strong correlations with the site occupancies. The geometry of the system was partly restrained under the following conditions: T-O $x=8=1.630(15)$ Å, O-O $x=12=2.661(25)$ Å, $M(1,2,3)-O$ $x=6=2.07(5)$ Å, $M(4)-O$ $x=8=2.55(20)$ Å. The weight associated with those observations was progressively reduced to 5 at the last stage of the refinement. Attempts to model the presence of preferred orientation using the generalized spherical-harmonic description of Von Dreele (1997) produced a small improvement of the fit as a result of a J texture index of 1.052. The number of terms was selected following Ballirano (2003). Convergence was reached at the agreement factors reported in Table 2; fractional coordinates and isotropic-displacement parameters are listed in Table 3, cell parameters in Table 4, selected bond distances in Table 5, cell parameters and site scattering (s.s.) values in Table 6. Experimental, calculated and difference plots are shown in Figure 3.

RESULTS AND DISCUSSION

EMP analysis by Fantauzzi et al. (2012) on fibre bundles, showed the chemical homogeneity of the fibres (Figure 4), with a mean composition corresponding to richterite (Table 7). In particular, the average crystal-chemical formula is very close to that intermediate between winchite and richterite $[^A A_{0.5} ^B NaCa ^C Mg_{4.5} M^{3+} _{0.5} ^T Si_8 O_{22} (OH)_2]$, where $M^{3+}=Fe^{3+}$ and/or Al, in agreement with previous studies (Sanchez et al., 2008; Gunter et al., 2003; Meeker et al.,

Table 2. Experimental details of the X-ray diffraction data collection and miscellaneous data for the refinement for the fibrous richterite from Libby. Statistical descriptors as defined by Young (1993).

Instrument	Bruker AXS D8 Advance
X-ray tube	CuK α at 40 kV and 40 mA
Incident beam optic	Multilayer X-ray mirrors
Sample mount	Rotating capillary (60 rpm)
Soller slits	2 (2.3° divergence + radial)
Divergence slit	0.8 mm
Detector	Position Sensitive Detector (PSD) VÄNTAC-1 opening window 6° 2θ
2θ range (°)	5-140
Step size (°)	0.02
Counting time (s)	10
R_p (%); R_{wp} (%); R_F (%)	1.75; 2.35; 6.48
Reduced χ^2	3.26
Restraints contribution to χ^2 (% of total χ^2)	375 (1.88)
Refined parameters	91
Peak-cut-off (%)	0.2
J	1.052
GU; GV; GW; LX	11(5); 99(5); 4.9(12); 5.47(14)
S/L=H/L	0.0153*
Richterite; microcline (wt%)	96.50(13); 3.50(13)

Note: * Kept fixed throughout the last stages of the refinement.

2003). However, the majority of the fibres show prevailing richterite and minor winchite components, in contrast to the reference data of amphiboles from Libby (Sanchez et al., 2008; Gunter et al., 2003; Meeker et al., 2003). It is worth noting that the chemical analysis of prismatic winchite (Gunter et al., 2003) and fibrous richterite (Fantauzzi et al., 2012) are similar except for a significantly higher F content in richterite than in winchite (0.82 apfu vs 0.37 apfu). The Fe^{3+}/Fe_{tot} ratio of richterite, determined by Mössbauer spectroscopy, is 65% (Fantauzzi et al., 2012). Briefly, Fe^{2+} was assigned to unresolvable band combinations of $[M(1)+M(3)]$ and $[M(2)+M(4)]$, and the amount of Fe^{2+} assigned to $[M(1)+M(3)]$ is about 80% of the total Fe^{2+} . The presence of Fe^{2+} at the $M(1)+M(3)$ sites is confirmed by the FT-IR spectrum (Figure 2). In fact, except for the typical absorption band at 3671 cm^{-1} assigned to arrangement $MgMgMg-OH$, a well-developed band is observed at 3658 cm^{-1} attributed to $M(1)+M(3)Fe^{2+}$ environment according to the results of Skogby and

Table 3. Fractional coordinates and isotropic displacement parameters (not refined) for fibrous richterite from Libby.

Site	x	y	z	U_{iso} (\AA^2)
O(1)	0.1128(6)	0.0860(3)	0.2170(10)	0.013
O(2)	0.1175(7)	0.1705(3)	0.7285(10)	0.014
O(3)	0.1071(8)	0	0.7136(13)	0.014
O(4)	0.3610(8)	0.2487(2)	0.8030(12)	0.015
O(5)	0.3451(8)	0.1313(2)	0.0926(10)	0.015
O(6)	0.3416(8)	0.1183(2)	0.5918(9)	0.014
O(7)	0.3299(9)	0	0.2877(14)	0.016
T(1)	0.2787(4)	0.08501(13)	0.2975(5)	0.011
T(2)	0.2855(4)	0.17101(13)	0.8038(5)	0.011
M(1)	0	0.0895(2)	0.5	0.009
M(2)	0	0.17958(18)	0	0.010
M(3)	0	0	0	0.020
M(4)	0	0.2764(2)	0.5	0.018
A(2/m)	0	0.5	0	0.105
H	0.214*	0*	0.775*	0.030

Note: * Kept fixed throughout the refinement.

Rossmann (1991) and Hawthorne and Della Ventura (2007). The $M(1)+M(3)Fe^{2+}$ occupancy calculated using the FT-IR data of Table 1 and following Burns and Strens (1966) is in very good agreement with that obtained by combining Mössbauer and EMP data (respectively $M(1)+M(3)Fe^{2+}=0.09$ apfu and 0.12 apfu). Fe^{3+} was allocated exclusively to $M(2)$ owing to the absence of absorption bands at $\Delta=-50\text{ cm}^{-1}$ from the tremolite reference band in the FT-IR spectrum (Raudsepp et al., 1987) possibly indicating the presence of $M(1)+M(3)Fe^{3+}$.

cell parameters of fibrous richterite are consistently smaller than those of prismatic winchite (Gunter et al., 2003) (Table 4). Cell parameters calculated according to

Table 4. Cell parameters of fibrous richterite from Libby. For comparison purposes, data of prismatic winchite from the same locality (G2003) (Gunter et al., 2003) are reported as well as the calculated cell parameters following Hawthorne and Oberti (2007).

	a (\AA)	b (\AA)	c (\AA)	β (°)
G2003	9.879(2)	18.024(3)	5.288(1)	104.377(3)
calculated	9.878(15)	17.997(11)	5.276(5)	104.554(8)
G2003				
Present work	9.8669(2)	17.9713(3)	5.27388(7)	104.3687(11)
calculated	9.884(15)	17.986(11)	5.276(5)	104.54(8)
present work				

Table 5. Selected bond distances (Å) fibrous richterite from Libby. Reference data of Gunter et al. (2003) (G2003) from single-crystal refinement are also reported for comparison. * Calculated $\langle M\text{-O} \rangle$ distances following Hawthorne and Oberti (2007).

	Libby	G2003	Libby	G2003	
T(1)-O(1)	1.586(5)	1.606(2)	T(2)-O(4)	1.583(5)	1.589(3)
T(1)-O(7)	1.614(3)	1.631(2)	T(2)-O(2)	1.606(5)	1.613(3)
T(1)-O(5)	1.625(5)	1.630(2)	T(2)-O(6)	1.661(5)	1.679(2)
T(1)-O(6)	1.635(5)	1.627(2)	T(2)-O(5)	1.652(5)	1.658(2)
$\langle T(1)\text{-O} \rangle$	1.615	1.624	$\langle T(2)\text{-O} \rangle$	1.626	1.635
$M(1)\text{-O(3) x 2}$	2.093(6)	2.091(2)	$M(2)\text{-O(4) x 2}$	1.978(6)	1.983(2)
$M(1)\text{-O(1) x 2}$	2.072(5)	2.067(2)	$M(2)\text{-O(2) x 2}$	2.060(6)	2.080(2)
$M(1)\text{-O(2) x 2}$	2.054(6)	2.068(2)	$M(2)\text{-O(1) x 2}$	2.178(5)	2.171(2)
$\langle M(1)\text{-O} \rangle$	2.073	2.075	$\langle M(2)\text{-O} \rangle$	2.072	2.078
<i>calculated*</i>	2.066	2.063	<i>calculated*</i>	2.075	2.081
$M(3)\text{-O(3) x 2}$	2.047(6)	2.058(3)	$M(4)\text{-O(4) x 2}$	2.393(6)	2.351(2)
$M(3)\text{-O(1) x 4}$	2.076(5)	2.080(2)	$M(4)\text{-O(2) x 2}$	2.393(6)	2.415(3)
$\langle M(3)\text{-O} \rangle$	2.066	2.073	$M(4)\text{-O(6) x 2}$	2.576(6)	2.564(2)
<i>calculated*</i>	2.064	2.067	$M(4)\text{-O(5) x 2}$	2.842(6)	2.836(2)
			$\langle M(4)\text{-O} \rangle$	2.551	2.542
$\langle A(2/m)\text{-O} \rangle$	2.933	2.937	<i>calculated*</i>	2.538	2.529

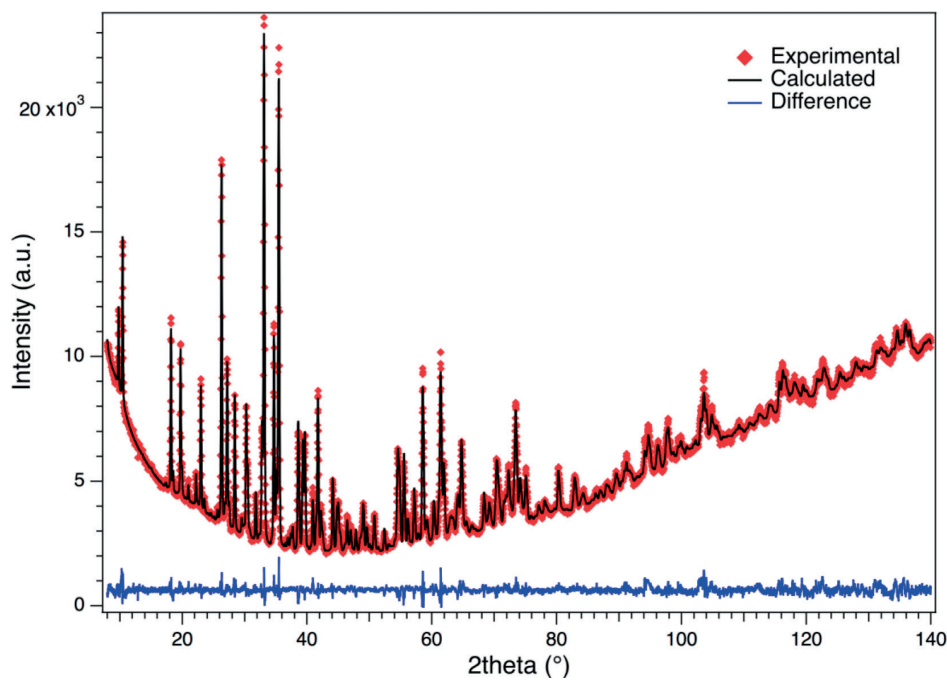


Figure 3. Rietveld plots of fibrous richterite from Libby.

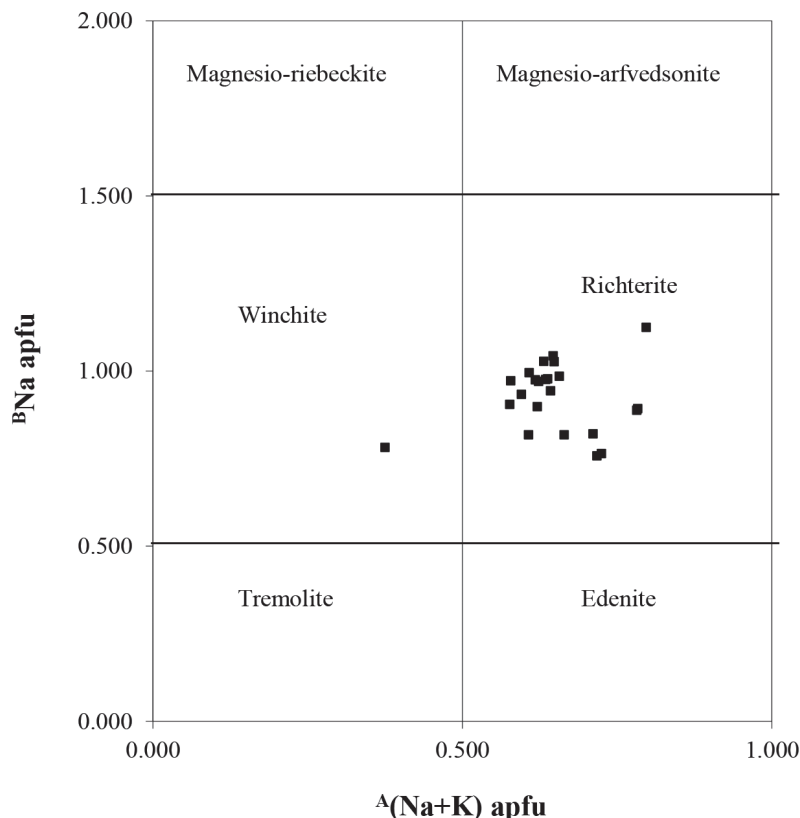


Figure 4. Composition of individual fibres of the richterite sample from Libby in the Leake's classification graph (Leake et al., 1997). Modified from Fantauzzi et al. (2012).

Table 6. Site-scattering (s.s) values (epfu*) for the fibrous richterite for Libby experimentally obtained from the structural refinement (left) and calculated from site occupancy (right). Possible site occupancy (central) is the result of combining chemical and Rietveld refinement data.

	s.s. from refinement	Possible site occupancy	s.s. from site occupancy
A	9.54(13)		9.19
<i>A</i> site sum	9.54(13)	Na _{0.362} ; K _{0.274}	9.19
M(4)	29.48(16)		
<i>B</i> site sum	29.48(16)	Ca _{1.063} ; Na _{0.937}	31.57
M(1)	23.02(14)	Mg _{1.920} ; Fe ²⁺ _{0.080}	25.12
M(2)	29.21(17)	Mg _{1.614} ; Fe ³⁺ _{0.301} ; Fe ²⁺ _{0.032} ; Cr _{0.025} ; Ti _{0.008} ; Al _{0.002} ; Mn _{0.018}	29.28
M(3)	12.05(11)	Mg _{0.950} ; Fe ²⁺ _{0.050}	12.70
<i>C</i> sites sum	64.28(42)		67.10
<i>A</i> + <i>B</i> + <i>C</i> sites sum	103.30(71)		107.86

* epfu: electrons per formula unit.

Table 7. Average chemical composition obtained by Electron Microprobe (23 analytical points) and the mean crystal-chemical formula of the fibrous richterite from Libby (recalculated from Fantauzzi et al., 2012). Data recalculated from Gunter et al. (2003) are reported for comparison purposes (G2003).

Oxides	Present work	G2003	Sites	Present work	G2003
	wt%	wt%		apfu	apfu
SiO ₂	57.53(37)	57.48(38)	Si	7.961	7.967
TiO ₂	0.08(4)	0.10(2)	^[4] Al	0.039	0.033
Al ₂ O ₃	0.25(10)	0.32(4)	ΣT	8.000	8.000
Cr ₂ O ₃	0.15(8)	-			
MgO	21.75(64)	21.43(23)	^[6] Al	0.002	0.019
CaO	7.16(70)	7.51(17)	Ti	0.008	0.010
MnO	0.15(5)	0.32(8)	Cr	0.025	-
FeO _{tot}	4.00(104)	4.59(13)	Fe ³⁺	0.301	0.343
Na ₂ O	4.84(45)	4.35(21)	Mg	4.488	4.429
K ₂ O	1.55(26)	1.08(5)	Fe ²⁺	0.162	0.189
F	1.88(27)	0.84(12)	Mn	0.020	0.010
Cl	0.01(1)	-	ΣC	5.004	5.000
H ₂ O*	1.26	1.77(5)			
			Mn	-	0.028
			Ca	1.063	1.115
	100.61	99.76	Na	0.937	0.857
F,Cl=O	0.79	0.35	ΣB	2.000	2.000
Total	99.82	99.41			
			Na	0.362	0.333
**Fe ₂ O ₃	2.89	3.29	K	0.274	0.191
**FeO	1.40	1.63	ΣA	0.636	0.524
			OH	1.163	1.637
			F	0.823	0.368
			Cl	0.002	-
			$\Sigma O(3)$	1.988	2.005

Note: *estimated from stoichiometry. **measured by ⁵⁷Fe Mössbauer spectroscopy.

the predictive equations of Hawthorne and Oberti (2007) are consistent with this trend. As mentioned above, the main chemical difference between fibrous richterite and prismatic winchite is related to a significantly higher F content of the former, which is expected to prevalently contribute to the cell contraction of richterite (see predictive equations reported in Table 12 of Hawthorne and Oberti, 2007). The $\langle T-O \rangle$ distance for fibrous richterite (1.621 Å) is slightly smaller than that of prismatic winchite (1.629 Å) (Table 5). In particular, $\langle T(1)-O \rangle$ (1.615 Å) and $\langle T(2)-O \rangle$ (1.626 Å) are among the mean shortest distances reported for *C2/m* amphiboles with ^[4]Al<0.06 apfu (see Fig. 15 in Hawthorne and Oberti, 2007).

The presence of tetrahedrally-coordinated Al (0.04 apfu) is confirmed by FT-IR investigation, due to the presence of the absorption band at 3706 cm⁻¹ (Figure 2) that indicates the presence of both ^{T(1)}Al and ^{O(3)}F (Hawthorne and Della Ventura, 2007). The observed $\langle M(1)-O \rangle$ (2.073 Å) $\langle M(2)-O \rangle$ (2.072 Å) and $\langle M(3)-O \rangle$ (2.066 Å) distances (Table 5) are in good agreement with those calculated using the equations of Hawthorne and Oberti (2007) (2.066 Å, 2.075 Å and 2.064 Å, respectively). The mean discrepancy is ca. 0.004 Å which is at the same level as the mean standard error of estimate of the three regression formulae (0.0046 Å) used for modelling the ^[6]M sites (Hawthorne and Oberti, 2007). It is worth noting that

the largest discrepancy between refined and calculated bond distances involves $\langle M(1)-O \rangle$ which has a smaller calculated value by 0.007 Å. The same behaviour is shown by prismatic winchite, which surprisingly shows a mean difference (0.007 Å) higher than that observed from XRPD data for fibrous richterite. The slight increase in $\langle M(4)-O \rangle$ distance observed for fibrous richterite with respect to prismatic winchite correlates with the higher $M^{(4)}Na$ content. In both cases, the calculated $\langle M(4)-O \rangle$ distance is 0.013 Å smaller than the refined distance. Nevertheless, the difference is at the same level as the mean standard error of estimate of the regression formula (0.011 Å) for $^{[8]}M$ (Hawthorne and Oberti, 2007). The total site scattering s.s. of the non-tetrahedral cation sites was calculated from the chemical data integrated with the Mössbauer analysis for iron valence. The site occupancy was obtained by combining the chemical data with the Rietveld-refinement results using the conventional assignment to the C group sites following Hawthorne (1981). It is worth noting that there is a discrepancy of -5% of the s.s. from structure refinement with respect to those from site occupancy (Table 6) for A, B and C group sites. This is in qualitative agreement with the findings of Vignaroli et al. (2014). Nevertheless, in the present case, within the C sites, almost all the discrepancy is taken up by $M(1)$, differently to $M(2)$ reported by Vignaroli et al. (2014). It has been suggested that this behaviour could be related to an imperfect absorption correction (Vignaroli et al., 2014). The present results support this hypothesis, as an increase in the capillary diameter with respect to that used in previous investigations (1 mm instead of 0.7 mm) has produced similar effects but distributed in a different way among the various A, B, and C group sites. The observed $\langle A-O \rangle$ distance in fibrous richterite is similar to that observed for the prismatic winchite. The difference between refined s.s. and those calculated from chemical data for the A site reaches ca. 4% relative (Table 6) and possibly partly reflects the simplified model used for the A site (a single site located at 0, ½, 0), which does not properly take into account the possible presence of electron density at the $A(m)$ and/or $A(2)$ sites.

LIBBY AMPHIBOLES: IMPLICATION

As a result of the high rates of respiratory diseases found in the miners of the now-closed vermiculite mine, the fibrous amphiboles occurring in the vermiculite deposit near Libby represent an environmental and health problem for the local citizens. Furthermore, it is worth noting that surface-reactivity investigation for fibrous richterite from Libby showed significant production of $HO\cdot$ radicals, which makes it potentially even more harmful than tremolite asbestos (Fantauzzi et al., 2012). However, in Libby, fibrous amphiboles are made of fibres forming solid-solution series, with an average

composition at the boundary between winchite and richterite, neither of which is regulated as asbestos. From a legal perspective, this finding makes it necessary to regulate both of the winchite-richterite series. Mazziotti-Tagliani et al. (2009) and Andreozzi et al. (2009) reported a similar case for amphibole fibres from Biancavilla (CT), Sicily, Italy. At this locality, amphibole fibres within altered volcanic rocks, mined for commercial purposes, were recognized as the cause of the anomalously high incidence of malignant mesothelioma in miners and/or local inhabitants. Fibres in Biancavilla are a solid-solution series with compositions ranging from fluoroedenite $[NaCa_2Mg_5Si_7AlO_{22}F_2]$ (dominant) to winchite $[\square NaCaMg_4(Al,Fe^{3+})Si_8O_{22}(OH)_2]$, with variable tremolite $[\square Ca_2(Mg,Fe^{2+})_5Si_8O_{22}(OH)_2]$ component. Very recently, fluoro-edenite has been included by IARC in the Group 1 Human-Carcinogens list (IARC, 2014, in press). These cases highlights the important role that mineralogical investigations play in the redefinition of non-regulated materials.

ACKNOWLEDGEMENTS

Prof. M.E. Gunter of the Department of Geological Sciences of the University of Idaho, USA, is thanked for the Libby richterite sample. Many thanks to Dr. M. Serracino for technical assistance with the EMP analyses at CNR-IGAG, UOS of Rome, Italy, and Prof. G. Della Ventura of the Department of Geological Sciences of the University of Roma Tre, Rome, Italy, for FT-IR data collection.

REFERENCES

Allan D.R. and Angel R.J. (1997) A high-pressure structural study of microcline ($KAlSi_3O_8$) to 7 GPa. European Journal of Mineralogy 9, 263-276.

Andreozzi G.B., Ballirano P., Gianfagna A., Mazziotti Tagliani S., Pacella A. (2009) Structural and spectroscopic characterization of a suite of fibrous amphiboles with high environmental and health relevance from Biancavilla (Sicily, Italy). American Mineralogist 94, 1333-1340.

Ballirano P. (2003) Effects of the choice of different ionization level for scattering curves and correction for small preferred orientation in Rietveld refinement: the $MgAl_2O_4$ test case. Journal of Applied Crystallography 36, 1056-1061.

Boettcher A.L. (1966) The Rainy Creek Alkaline-ultramafic complex near Libby, Montana. PhD thesis, Pennsylvania State University, 155 pp.

Burns R.G. and Strens R.G.J. (1966) Infrared study of the hydroxyl bands in clinoamphiboles. Science 153, 890-892.

Fantauzzi M., Pacella A., Fournier J., Gianfagna A., Andreozzi G.B., Rossi A. (2012) Surface chemistry and surface reactivity of fibrous amphibole that are not regulated as asbestos. Analytical and Bioanalytical Chemistry 404, 821-833.

Finger L.W., Cox D.E., Jephcoat A.P. (1994) A correction for powder diffraction peak asymmetry due to axial divergence. Journal of Applied Crystallography 27, 892-900.

Fubini B. (1993) The possible role of surface chemistry in the toxicity of inhaled fibers. In: Fiber Toxicology. (ed): D.B.

Wahreit, Academic Press, San Diego (USA), 11, 229-257.

Fubini B. (1996) Use of physico-chemical and cell free assays to evaluate the potential carcinogenicity of fibres. In: Mechanisms of Fibre Carcinogenesis. (eds): A.B. Kane, P. Boffetta, R. Saracci, J. Wilbourn, IARC Scientific Publication, Lyon (France), 140, 35-54.

Fubini B., Fenoglio I., Elias Z., Poirot O. (2001) On the variability of the biological responses to silicas: effect of origin, crystallinity and state of the surface on the generation of reactive oxygen species and consequent morphological transformations in cells. *Journal of Environmental Pathology, Toxicology and Oncology* 20, 87-100.

Fubini B. and Otero Aréan C. (1999) Chemical aspects of the toxicity of inhaled mineral dusts. *Chemical Society Reviews* 28, 373-381.

Gunter M.E., Brown B.M., Bandli B.R., Dyer M.D. (2001) Amphibole asbestos, vermiculite mining and Libby, Montana: What's in a name? (abstract #3455): Eleventh Annual V.M., Goldschmidt Conference, Hot Springs, Virginia.

Gunter M.E., Dyer M.D., Twamley B., Foit F.F. Jr., Cornelius C. (2003) Composition, Fe^{3+}/SFe , and crystal structure of non-asbestiform and asbestiform amphiboles from Libby, Montana, U.S.A. *American Mineralogist* 88, 1970-1978.

Hawthorne F.C. (1981) Crystal chemistry of the amphiboles. In: *Amphiboles and other hydrous pyroboles mineralogy*. Reviews in Mineralogy. (ed.): D.R. Veblen., Mineralogical Society of America, Chantilly (USA) 9A, 1-102.

Hawthorne F.C. and Della Ventura (2007) Short range order in amphiboles. In: *Amphiboles: Crystal chemistry, occurrence, and health issues*. Reviews in Mineralogy and Geochemistry. (eds): F.C. Hawthorne, R. Oberti, G. Della Ventura, A. Mottana, Mineralogical Society of America, Chantilly (USA) 67, 173-222.

Hawthorne F.C. and Oberti R. (2007) Amphiboles: Crystal chemistry. In: *Amphiboles: Crystal chemistry, occurrence, and health issues*. Reviews in Mineralogy and Geochemistry. (eds): F.C. Hawthorne, R. Oberti, G. Della Ventura, A. Mottana, Mineralogical Society of America, Chantilly (USA) 67, 1-54

Hawthorne F.C., Oberti R., Zanetti A., Nayak V.K. (2008) The crystal chemistry of alkali amphiboles from Kajlidongri manganese mine, India. *Canadian Mineralogist* 46, 455-466.

IARC (in press) Fluoro-edenite, silicon carbide fibres and whiskers, and single-walled and multi-walled carbon nanotubes. IARC Monographs on the evaluation of the carcinogenic risk to humans, 111.

IARC (2014) Carcinogenicity of fluoro-edenite, silicon carbide fibres and whiskers, and carbon nanotubes. *Lancet Oncology* 15, 1427-1428.

Larson A.C. and Von Dreele R.B. (1985) General Structure Analysis System (GSAS). Los Alamos National Laboratory Report (LAUR 86-748), Los Alamos, New Mexico 224 pp.

Leake B.E., Woolley A.R., Arps C.E.S., Birch W.D., Gilbert M.C., Grice J.D., Hawthorne F.C., Kato A., Kisch H.J., Krivovichev V.G., Linthout K., Laird J., Mandarino J.A., Maresch V.W., Nickel E.H., Rock N.M.S., Schumacher J.C., Smith D.C., Stephenson N.N., Ungaretti L., Withtaker E.J.W., Youzhi G. (1997) Nomenclature of amphiboles: report of the subcommittee on amphiboles of the International Mineralogical Association, Commission on New Minerals and Mineral Names. *American Mineralogist* 82, 1019-1037.

Mazzotti Tagliani S., Andreozzi G.B., Bruni B.M., Gianfagna A., Pacella A., Paoletti, L. (2009) Chemical variability of a suite of fibrous amphiboles from Biancavilla (Sicily, Italy). *Periodico di Mineralogia* 78, 65-74.

McDonald J.C., McDonald A.D., Armstrong B., Sébastien P. (1986) Cohort study of mortality of vermiculite miners exposed to tremolite. *British Journal of Industrial Medicine* 43, 436-444.

McDonald J.C., Harris J., Armstrong B (2001) Cohort mortality study of vermiculite miners exposed to fibrous tremolite: an update (abstract). *Inhaled Particles*, Robinson College, Cambridge, United Kingdom, September 2-6.

Meeker G.P., Bern A.M., Brownfield I.K., Lowers H.A., Sutley S.J., Hoefen T.M., Vance J.S. (2003) The composition and morphology of amphiboles from the Rainy Creek Complex, near Libby, Montana. *American Mineralogist* 88, 1955-1969.

Pacella A., Fantauzzi M., Turci F., Cremisini C., Montereali M.R., Nardi E., Atzei D., Rossi A., Andreozzi G.B. (2015) Surface alteration mechanism and topochemistry of iron in tremolite asbestos: a step toward the understanding of amphibole asbestos potential hazard. *Chemical Geology* 405, 28-38.

Pardee, J.T. and Larsen E.S. (1928) Deposits of vermiculite and other minerals in the Rainy Creek District, near Libby, Mont. In Contributions to economic geology, U.S. Geological Survey Bulletin 805, 17-29.

Raudsepp M., Turnock A.C., Hawthorne F.C., Sherriff B.K., Hartman J.S. (1987) Characterization of synthetic pargasitic amphiboles ($NaCa_2Mg_3^{+}Si_6Al_2O_{22}(OH,F)_2$; $M^{3+}=Al, Cr, Ga, Sc, In$) by infrared spectroscopy, Rietveld structure refinement, and ^{27}Al , ^{29}Si , and ^{19}F MAS NMR spectroscopy. *American Mineralogist* 72, 580-593.

Sanchez M.S., Gunter M.E., Dyer M.D. (2008) Characterization of historical amphibole samples from the former vermiculite mine near Libby, Montana, U.S.A. *European Journal of Mineralogy* 20, 1043-1053.

Skogby H. and Rossman G.R. (1991) The intensity of amphibole OH bands in the Infrared absorption spectrum. *Physics and Chemistry of Minerals* 18, 64-68.

Thompson P., Cox D.E., Hastings J.B. (1987) Rietveld refinement of Debye-Scherrer synchrotron X-ray data from Al_2O_3 . *Journal of Applied Crystallography* 20, 79-83.

Toby B.H. (2001) EXPGUI, a graphical user interface for GSAS. *Journal of Applied Crystallography* 34, 210-213.

Vignaroli G., Ballirano P., Belardi G., Rossetti F. (2014) Asbestos fibre identification vs. evaluation of asbestos hazard in ophiolitic rock mélange, a case study from the Ligurian Alps (Italy). *Environmental Earth Sciences* 72, 3679-3698.

Von Dreele R.B. (1997) Quantitative texture analysis by Rietveld refinement. *Journal of Applied Crystallography* 30, 517-525.

Wilye A. and Verkouteren J. (2000) Amphibole asbestos from Libby, Montana: aspects of nomenclature. *American Mineralogist* 85, 1540-1542.

Young R.A. (1993) Introduction to the Rietveld method. In: The Rietveld method. (ed.): R.A Young, Oxford Science, Oxford 1-38.